1521-0111/12/8101-21–30$25.00
MOLECULAR PHARMACOLOGY
Copyright © 2012 The American Society for Pharmacology and Experimental Therapeutics
Mol Pharmacol 81:21–30, 2012

Vol. 81, No. 1
75234/3737533

The LRRC26 Protein Selectively Alters the Efficacy of BK Channel Activators

Janos Almassy and Ted Begenisich

Department of Pharmacology and Physiology, University of Rochester School of Medicine and Dentistry, Rochester, New York

Received August 12, 2011; accepted October 7, 2011

ABSTRACT

Large conductance, Ca^{2+}-activated K channel proteins are involved in a wide range of physiological activities, so there is considerable interest in the pharmacology of large conductance calcium-activated K (BK) channels. One potent activator of BK channels is mallotoxin (MTX), which produces a very large hyperpolarizing shift of the voltage gating of heterologously expressed BK channels and causes a dramatic increase in the activity of BK channels in human smooth muscle cells. However, we found that MTX shifted the steady-state activation of BK channels in native parotid acinar cells by only 6 mV. This was not because the parotid BK isoform (parSlo) is inherently insensitive to MTX as MTX shifted the activation of heterologously expressed parSlo channels by 70 mV. Even though MTX had a minimal effect on steady-state activation of parotid BK channels, it produced an approximate 2-fold speeding of the channel-gating kinetics. The BK channels in parotid acinar cells have a much more hyperpolarized voltage activation range than BK channels in most other cell types. We found that this is probably attributable to an accessory protein, LRRC26, which is expressed in parotid glands: expressed parSlo + LRRC26 channels were resistant to the actions of MTX. Another class of BK activators is the benzimidazalones that includes 1,3-dihydro-1-(2-hydroxy-5-(trifluoromethyl)phenyl)-5-(trifluoromethyl)-2*H*-benzimidazol-2-one (NS-1619). Although the LRRC26 accessory protein strongly inhibited the ability of MTX to activate BK channels, we found that it had only a small effect on the action of NS-1619 on BK channels. Thus, the LRRC26 BK channel accessory protein selectively alters the pharmacology of BK channels.

Introduction

Potassium-selective ion channel proteins form the largest and most diverse class of ion channels. Most of these channels are composed of four identical subunits assembled to provide a narrow potassium-selective pore, and the crystal structures of several of these have been solved (Doyle et al., 1998; Jiang et al., 2002; Long et al., 2005). BK (or maxi-K) channels are unique members of this very large class in that they are activated by both membrane voltage and by a ligand, Ca^{2+}. At negative potentials and at low Ca^{2+} levels, these channels are closed. Depolarization, sensed by positively charged amino acid residues in the fourth membrane-spanning (S4) domain of each channel subunit, increases the channel open probability (e.g., Diaz et al., 1998). Ca^{2+} binds to a region in the very large C terminus of each subunit and produces a hyperpolarizing shift in channel activation. The cooperative interplay between membrane potential and Ca^{2+} has been the subject of extensive study for many years (Horrigan and Aldrich, 1999; Horrigan et al., 1999; Rothberg and Magleby, 1999, 2000; Magleby, 2003). These efforts have culminated in a concise and quantitative description of the allosteric gating properties of BK channels: the Horrigan-Aldrich (H-A) model (Horrigan and Aldrich, 2002).

In addition to their unique ability to be activated by both voltage and Ca^{2+}, BK channels are modulated by a variety of endogenous signaling molecules. It is probable that as a result of these special properties, BK channels are widely distributed in the body and play a variety of important physiological roles. They are involved in fluid and electrolyte secretion (e.g., Romanenko et al., 2006), control of smooth muscle contraction (Brayden and Nelson, 1992), and control of electrical activity in many regions of the brain (reviewed in Salkoff et al., 2006). Because of their prominent physiological roles BK channels have been actively targeted for the development of therapeutic compounds (e.g., Garcia et al., 1995, 2007; Gribkoff et al., 2001; Jensen et al., 2003; Marx and Zakharov, 2006; Nardi and Olesen, 2008). One class of potentially therapeutic drugs increases the activation of BK-

This work was supported by National Institutes of Health National Institute of Dental and Craniofacial Research [Grants R01-DE016960, R01-DE019245].

Article, publication date, and citation information can be found at http://molpharm.aspetjournals.org.

http://dx.doi.org/10.1124/mol.111.075234.

ABBREVIATIONS: BK, large conductance calcium-activated potassium channel; MTX, mallotoxin; parSlo, native parotid Slo gene; H-A model, Horrigan-Aldrich BK channel allosteric gating model; NS-1619, 1,3-dihydro-1-(2-hydroxy-5-(trifluoromethyl)phenyl)-5-(trifluoromethyl)-2*H*-benzimidazol-2-one.

even at relatively negative membrane voltages. Many such compounds have been identified, and most of these act by producing a hyperpolarizing shift of channel activation (reviewed by Gribkoff et al., 1997). One class of such activators is the benzimidazalones exemplified by NS-1619 and its structural analogs (Strøbaek et al., 1996). A very powerful addition to the list of BK-modulating compounds has recently been identified: mallotoxin (rottlerin), a liphophilic product isolated from a powder covering the capsules of the Mallotus Phillippinensis tree. Concentrations of mallotoxin (MTX) in the micromolar range shift BK channel activation by more than 100 mV (Zakharov et al., 2005). These large effects of MTX occur on native BK channels in human smooth muscle cells as well as heterologously expressed channels. Both the benzimidazalones and MTX have been proposed for therapeutic uses (Teuber et al., 2003; Marx and Zakharov, 2006).

As noted above, BK channels are involved in fluid and electrolyte secretion in tissues such as salivary glands. Defects in fluid secretion underlie several pathological conditions, including oral pain, increased dental caries, and infections by opportunistic microorganisms such as *Candida albicans*. It is possible that activation of potassium channels in these cells would promote fluid secretion and that so BK activators could have therapeutic value in salivary gland pathologies. We tested MTX on BK channels in mouse parotid acinar cells and, contrary to the findings described above, found a negligible effect of this compound on the voltage dependence of steady-state activation. We investigated the reasons for the lack of effectiveness of this activator on parotid BK channels and found that a recently identified accessory protein, LRRC26 (Yan and Aldrich, 2010), caused BK channels to lose their sensitivity to the gating shift of MTX. We tested the specificity of the LRRC26 accessory protein by examining the action of another BK channel activator, NS-1619, on BK channels with and without the protein. We found a minimal effect of the accessory protein on the effectiveness of NS-1619. Thus, the LRRC26 accessory protein can selectively control the sensitivity of BK channels to channel modulators.

Materials and Methods

Parotid Acinar Cell Preparation. Single acinar cells were enzymatically isolated from CD-1 mouse parotid glands with techniques that have previously been described in detail (Thompson and Begenisich, 2006). All animals used in this study were housed in a pathogen-free area at the University of Rochester, and all procedures for animal handling, maintenance, and surgery were approved by the University of Rochester Committee on Animal Resources.

Cell Culture and Heterologous Expression. The mouse parotid $K_{Ca}1.1$ variant (parSlo; see Nehrke et al., 2003) was cotransfected (~0.8 μg) into CHO-K1 cells using a Nucleofector machine (Amaxa Biosystems, Gaithersburg, MD) according to the manufacturer's instructions along with 0.1 μg of the fluorescent vector EYFP-pdc315 for transfected cell identification and with or without 0.5 μg of human LRRC26 in pCMV6-XL5 (Origene, Rockville, MD). Cells were used 24 h after transfection. CHO-K1 cells were obtained from American Type Culture Collection (Manassas, VA) and grown in Ham's F-12K medium + L-glutamine (American Type Culture Collection) with 10% fetal bovine serum and maintained in a CO_2 incubator with 5% CO_2.

Solutions. Two external (bath) solutions were used. One solution (5-K) was designed to mimic physiological cation conditions and contained 135 mM sodium glutamate, 5 mM potassium glutamate, 2 mM $CaCl_2$, 2 mM $MgCl_2$, and 10 mM HEPES, pH 7.2. The use of glutamate rather than chloride allowed the measurement of potassium currents from the parotid acinar cells without significant contribution from the native chloride channels in these cells. A second external solution (Hi-K) contained 135 mM potassium glutamate, 2 mM $CaCl_2$, 2 mM $MgCl_2$, and 10 mM HEPES, pH 7.2. The nominally "0" Ca^{2+} internal solution contained 135 mM potassium glutamate buffered to pH 7.2 with 10 mM HEPES and 10 mM 1,2-bis(2-aminophenoxy)ethane-*N*,*N*,*N*′,*N*′-tetraacetic acid, with no added Ca^{2+}. In some experiments, we used an internal solution designed to contain 10 μM free Ca^{2+} (135 mM potassium glutamate, 5 mM *N*-hydroxyEDTA, 3.6 mM $CaCl_2$, and 10 mM HEPES, pH 7.2).

Parotid acinar cells express two types of Ca^{2+}-activated potassium channels: BK and IK1 (Nehrke et al., 2003). IK1 channels are not activated at low Ca^{2+} levels (Ishii et al., 1997; Romanenko et al., 2010), and our experiments with parotid cells were done with the zero Ca^{2+} solution. Thus, IK1 channels will not interfere with our measurements of BK channel currents from the parotid cells. The lack of IK1 currents in our measurements can be seen by the absence of a significant time-independent component in the raw currents records of Fig. 1—a hallmark of IK1 channels (e.g., Ishii et al., 1997). Mallotoxin (rottlerin) and NS-1619 were purchased from Sigma-Aldrich (St. Louis, MO), stored at −20 C° in aliquots in dimethyl sulfoxide and diluted to produce the final working concentrations.

Electrophysiological Recordings. Whole-cell currents were acquired at room temperature using Axopatch 200B amplifier and Digidata 1320A digitizer (Molecular Devices, Sunnyvale, CA) at a 50-kHz sampling rate and filtered online at 5 kHz using a low-pass Bessel filter. Patch pipettes were made from quartz (Garner Glass Co., Claremont, CA) or borosilicate glass (Warner Instruments, Hamden, CT) with typical resistance values between 3 and 6 MΩ. A minimal value of 90% series resistance compensation was used with most values near 95%. Voltage clamp steps were 100 or 150 ms in duration from a −60- or −70-mV holding potential except in experiments with expressed parSlo in the absence of Ca^{2+} where a holding potential of +30 mV was used to allow depolarizations beyond 200 mV. With this high-voltage, whole-cell protocol, it was difficult to maintain a tight seal, so in most cases the data in the absence and presence of the activators were obtained from separate cells. Single channel activity was measured with the Hi-K solution in whole-cell mode.

Data Analysis. The voltage dependence of channel activation was estimated from steady-state conductance as $I_{SS}/(V_m - V_K)$, where V_K is the K^+ equilibrium potential. These conductance-voltage relations were fit by the Boltzmann equation: $G(V_m) = G_{max}/(1 + \exp[-z(V_m - V_h)F/RT])$, where z is the effective valence that controls the voltage sensitivity (steepness) of activation; V_h is the voltage at half-activation; F is the Faraday constant; R is the gas constant; and T is absolute temperature. Relative activation was computed by normalizing the conductance values by the maximal level obtained from the fit. Important constraints for analysis of BK channel properties with the H-A model (see *Discussion*) require channel activation data at very low open probabilities in nominally Ca^{2+}-free internal solutions. Thus, the data from the H-A analysis (Fig. 7) were obtained with the Hi-K solution. BK channel activation at positive potentials was estimated as relative conductance from whole-cell steady-state currents. At negative potentials, we measured single channel activity in whole-cell mode and determined the channel fractional open time. The measured single channel conductance and the maximal whole-cell conductance for that cell were used to compute the open probability.

Single exponential time functions were fit to the time course of current activation to obtain channel gating time constants. These fits were done using Clampfit 9.2 or software of our own design using the Simplex Algorithm. The voltage dependence of these time constants was fit by the expectation of a single open-closed transition with

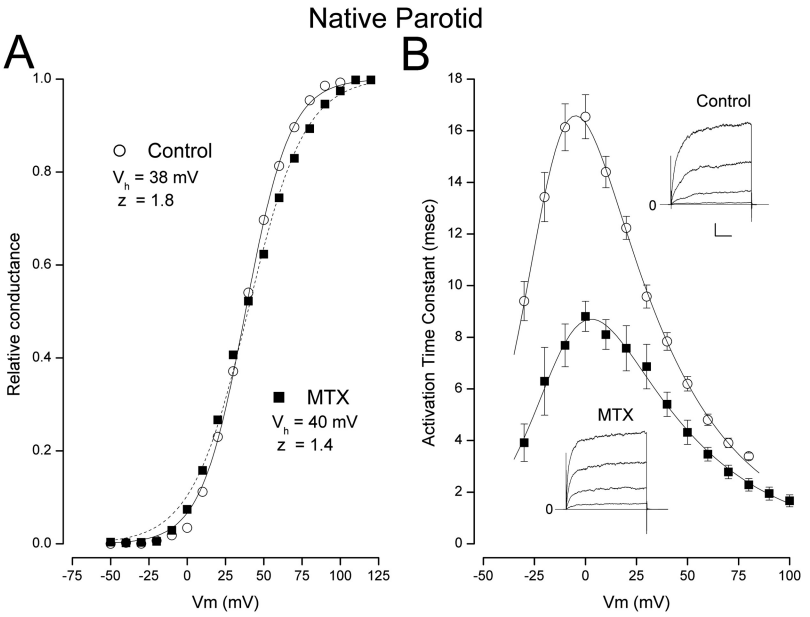

Fig. 1. MTX action on BK channels in native parotid cells. A, voltage dependence of relative BK conductance in a representative mouse parotid acinar cell in the absence (○) and presence (■) of 5 μM MTX. Lines, fits of the Boltzmann equation (see *Materials and Methods*) with the indicated parameters. B, voltage dependence of activation time constant. Pooled data in the absence (○, N = 8–15) and presence (■) of 5 μM MTX (N = 6–7 except at −30 mV with N = 2). Solid lines are fits of eq. 1 (see *Materials and Methods*) to the data. Insets, raw current data from a cell in the absence and presence of MTX as indicated. Voltages of 0, 20, 40, and 60 mV. Calibration, 1 nA, 20 ms.

voltage-dependent, forward and backward rate constants a and b, respectively:

$$\text{Time Constant} = 1/(a + b)$$

where

$$a = a_0 \cdot \exp(z_a V_m F/RT) \text{ and } b = b_0 \cdot \exp(z_b V_m F/RT) \quad (1)$$

fits of the Boltzmann equation and eq. 1 were made in Origin 6.1. Mean values are reported with mean ± S.E.M. values.

Previous studies have revealed significant patch to patch variability in the half-activation voltage of heterologously expressed Slo channels (Stefani et al., 1997; Horrigan et al., 1999), possibly the result of variable redox states (DiChiara and Reinhart, 1997). Computing mean voltage-activation relations with such variability distorts the shape of the relation such that it no longer reflects the true voltage sensitivity. To deal with this issue, some authors (e.g., Horrigan and Aldrich, 2002; Orio and Latorre, 2005) have chosen to shift the activation curves from multiple cells so that the half-activation voltage from each cell coincides with the overall mean value and, through an interpolation procedure, compute a mean voltage-activation relation. With the exception of the H-A analysis of expressed parSlo in Fig. 7, we chose to simply report the mean V_h and z values from fits of the Boltzmann equation. This issue is exacerbated by the inevitable variability of the shift produced by MTX, so for the H-A analysis of MTX-treated parSlo BK channels, we chose to use activation data at positive potentials from a single cell that had V_h and z values very close to the mean values. Part of the H-A analysis uses single channel open-probability measurements at very negative potentials where the distorting effect is less problematic. Therefore, for that analysis, we used mean activation values from several cells. The H-A analysis was done in Origin 6.1. Under normal conditions in zero Ca^{2+}, the H-A V_J parameter (see *Discussion*) is quite similar to the voltage at which the activation time constant achieves its maximal value (Horrigan and Aldrich, 2002); thus, for our H-A analysis of expressed parSlo BK channels, we constrained V_J to be within 20 mV of this value (Fig. 2B). The z parameters were constrained to be between 0 and 2. Parameter seed values for the fitting algorithm were those from our previous similar analysis (Romanenko et al.,

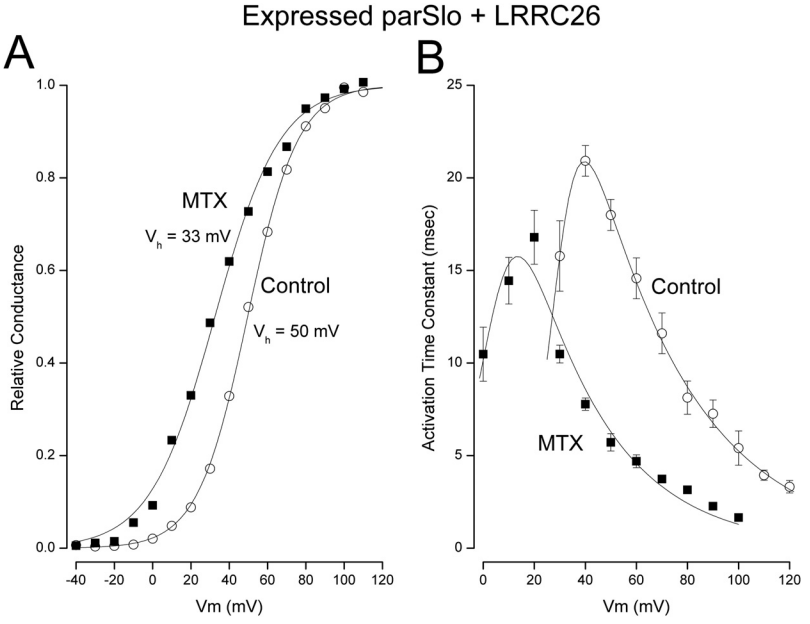

Fig. 2. MTX shifts activation of heterologously expressed parotid BK channels. A, voltage dependence of relative BK conductance in the absence (○) and presence (■) of 5 μM MTX. Solid lines, fits of the Boltzmann equation (see *Materials and Methods*) with the indicated parameters. Insets, raw BK currents in the absence (voltages, 60, 80, 100, 120, 140, and 160 mV) and presence (voltages, 120, 140, 160, 180, and 200 mV) of 5 μM MTX as indicated. For each condition, the smallest detectable current and the associated voltage are indicated. Calibration, 2.5 nA, 20 ms (Control); 1 nA, 20 ms (MTX). B, voltage dependence of activation time constant. Pooled data in the absence (○, N = 5–19) and presence (■) of 5 μM MTX (N = 4–10). Solid lines are fits of eq. 1 (see *Materials and Methods*) to the data.

2010). For the analysis of the MTX-treated channels (Fig. 7B), the z parameters were fixed at the values from the fit to the control data, and the V_J value was constrained to be within 20 mV of the voltage at which the activation time constant achieved its maximal value (100 mV; see Fig. 2B).

Results

As described in the Introduction, the compound MTX exerts a powerful effect on BK channel activation by producing a very large hyperpolarizing shift in the voltage dependence of channel activation (Zakharov et al., 2005). Thus, various pathologies, including those associated with salivary gland hypofunction, could be improved by such a compound. As a first step in evaluating MTX as a possible therapeutic treatment for hyposalivation, we tested its action on BK channels in mouse parotid acinar cells. Since any such therapeutic agent would need to act on intact cells under physiological conditions, we used whole-cell recordings with physiological potassium concentrations (see *Materials and Methods*): 5 and 135 mM for extracellular and intracellular potassium, respectively. BK channels are activated both by voltage and by intracellular Ca^{2+}; however, to simplify analysis, we initially used intracellular solutions with Ca^{2+} chelated to near zero levels (see *Materials and Methods*).

MTX Action on BK Channels in Parotid Acinar Cells. As illustrated in Fig. 1A, 5 μM MTX had only a very small effect on the voltage dependence of steady-state activation of native BK channels in parotid acinar cells under these physiological conditions. The figure illustrates the voltage dependence of parotid BK channel activation, computed as conductance from whole-cell currents in the absence (○) and presence of 5 μM MTX (■). The solid lines are fits of the Boltzmann equation from which the activation midpoint voltage, V_h, and effective valence (or steepness), z, were obtained (see *Materials and Methods*). MTX treatment had a minimal effect on the voltage dependence of BK. The V_h value for the control cell was ~38 mV, and that for the MTX-treated cell was ~40 mV. There also appeared to be a small decrease in the voltage sensitivity of activation as judged by a slight decrease in the z parameter. The minimal effect on the half-activation voltage, V_h, and the small decrease in voltage sensitivity, z, were consistent findings: the mean V_h value was 42 ± 1.4 mV for 16 control cells and 36 ± 2.8 mV for 8 cells treated with 5 μM MTX. The mean z parameter decreased with MTX treatment from 1.7 ± 0.04 to 1.4 ± 0.05. The small hyperpolarizing shift in V_h and small decrease in z were both significant at the $p = 0.05$ level. Thus, MTX treatment produced only a small (6 mV) hyperpolarizing shift of parotid BK channel activation and a modest decrease in the voltage sensitivity of channel activation. These findings are summarized in Table 1.

The data in Fig. 1B show that the inability of MTX to affect the voltage dependence of native parotid BK channels was not the results of an inability of MTX to interact with the channel. The insets contain raw current traces from a cell in the absence (Control) and presence of MTX as indicated. It is clear that MTX increased the speed of activation of these native BK channels. The main figure (Fig. 1B) contains pooled time constant data obtained in the absence (○) and presence (■) of 5 μM MTX. Treatment with MTX produced an approximate 2-fold decrease in the activation time constant, with little or no shift of its voltage dependence.

TABLE 1
Summary of BK channel activation parameters

	V_h	z	N
	mV		
Parotid			
Control	42 ± 1.4	1.7 ± 0.04	16
MTX	36 ± 2.8	1.4 ± 0.05	8
Shift	6		
parSlo			
Control	188 ± 2.0	1.2 ± 0.04	5
MTX	118 ± 4.3	1.2 ± 0.04	8
Shift	70		
parSlo + LRRC26			
Control	52 ± 2.0	2.1 ± 0.05	7
MTX	35 ± 3.6	1.5 ± 0.11	6
Shift	17		

The very small effect of MTX on the voltage dependence of parotid BK channel activation was quite surprising, because a 10-fold lower concentration (0.5 μM) has been reported to produce a 100-mV shift of heterologously expressed BK channels and a dramatic increase in activity of BK channels in human smooth muscle cells (Zakharov et al., 2005). This discrepancy could potentially be the result of differences between the parotid BK channel isoform (Nehrke et al., 2003) and the mSlo1 clone used in the heterologous expression experiments of Zakharov et al. (2005). However, as noted above, Zakharov et al. (2005) also found strong effects of MTX on the BK channels in human smooth muscle and that the parotid isoform is rather similar to hSlo in that it differs at only five individual and the last eight conceptually translated amino acids (see alignment in Nehrke et al., 2003). Nevertheless, to more rigorously test for a possible isoform-specific action, we assessed the effect of MTX on heterologously expressed parotid BK (parSlo) channels and illustrated an example of the results in Fig. 2.

MTX on Heterologously Expressed parSlo BK Channels. The insets of Fig. 2A contains examples of whole-cell BK currents recorded from a control cell and from a cell treated with 5 μM MTX as indicated. The control currents (bottom inset) were recorded at potentials from 120 to 220 mV in 20-mV increments and from 60 to 160 mV for the MTX data (top inset). As indicated by the arrows, a depolarization to near 120 mV was necessary to elicit detectable BK current in the absence of MTX, but only 60 mV was needed in the presence of MTX.

The open circles in the main plot of Fig. 2A illustrate the voltage dependence of BK channel activation as determined from the relative conductance-voltage relation (see *Materials and Methods*). As is typical of heterologously expressed BK channels in low Ca^{2+} in the absence of auxiliary subunits or other modulation factors, activation occurs only at very large depolarizations (Butler et al., 1993). The solid line is a fit of the Boltzmann relation to the data from which it can be determined that a depolarization to 189 mV was required to activate half of the channels. Treatment with 5 μM MTX allowed the channels to activate at much smaller depolarizations, with a V_h of 116 mV (■): a 73-mV hyperpolarizing shift. The mean V_h value from five control cells was 188 ± 2.0 and 118 ± 4.3 mV from eight MTX-treated cells. The steepness of the activation curve (as indicated by the Boltzmann z parameter) was unchanged: a mean value of 1.2 ± 0.04 for both control and MTX-treated cells. Thus, 5 μM MTX produced a very large, 70-mV hyperpolarizing shift of the voltage depen-

dence of expressed parSlo BK channel activation. In addition, the data in Fig. 2B show that MTX appeared to produce a similar (~80 mV) hyperpolarizing shift in the voltage dependence of the activation time constant with little or no change in the peak time constant value. These very large effects of MTX on the expressed parotid BK channel are consistent with the findings of Zakharov et al. (2005) and show that the expressed parSlo isoform was certainly sensitive to MTX treatment. Consequently, there must be some special property of BK channels in native parotid acinar cells that alters their response to MTX.

ParSlo + LRRC26 BK Channels. A comparison of the control data in Figs. 1A and 2A shows that native parotid BK channels activate at potentials of ~150 mV more hyperpolarized than the same channels in the heterologous expression system. In many types of cells, BK channels (at low intracellular Ca^{2+} levels) need very large depolarizations for activation (see review by Latorre et al., 1989) just as required for the heterologously expressed parSlo channels illustrated in Fig. 2. In contrast, BK channels in parotid (see Fig. 1A) and submandibular (Romanenko et al., 2007) salivary glands can be activated at relatively negative voltages. A few other cell types share this property, including mammalian inner hair cells (Thurm et al., 2005) and prostate cancer cells (Gessner et al., 2005). It was recently shown that a BK channel auxiliary protein (LRRC26) is responsible for the hyperpolarized activation of the BK channels in these prostate cancer cells (Yan and Aldrich, 2010). In addition to the prostate, LRRC26 is also highly expressed in normal salivary glands and at low levels in colon, pancreas, and intestine (Egland et al., 2006). In addition, the LRRC26 protein was found in human parotid exosomes along with TMEM16A and NKCC1, proteins that are primarily, if not exclusively, expressed in acinar cells (Gonzalez-Begne et al., 2009). These findings lead us to postulate that the hyperpolarized activation range of parotid acinar cell BK channels was attributed to their association with the LRRC26 protein. We tested this possibility by coexpressing parotid BK channels and the human LRRC26 protein; an example of the results is illustrated in Fig. 3.

The expressed parSlo data in the absence of MTX from Fig. 2 are replotted in Fig. 3 (○) along with data (■) from a cell coexpressing parSlo and the LRRC26 protein. As noted above, very large depolarizations were required to activate channels formed only of parSlo subunits. The results in Fig. 3A show that parSlo channels associated with the LRRC26 channel were activated at potentials of ~140 mV more negative than channels formed by only the parSlo subunits. There was also an increase in the steepness of the voltage dependence of steady-state activation as indicated by an increase in the z parameter. The effects of LRRC26 expression on parSlo steady-state activation are summarized in Table 1. LRRC26 expression resulted in a similar hyperpolarizing shift of the voltage dependence of channel gating kinetics and an almost 2-fold slowing of the maximal time constant value as illustrated in Fig. 3B. Representative raw currents are illustrated in the insets, and the slower kinetics of the channels with the LRRC26 protein is evident. These findings are quite similar to those recently reported for the actions of LRRC26 on mSlo channel gating (Yan and Aldrich, 2010).

MTX Action on ParSlo + LRRC26 BK Channels. The results illustrated in Fig. 3 show that, as predicted, coexpression of LRRC26 resulted in BK channels with gating properties much more like the channels in native parotid cells than channels consisting of only the parSlo subunit. We next tested our hypothesis that the very different effects of MTX on native parotid and expressed parSlo BK channels could be accounted for by the LRRC26 protein. Thus, we examined the actions of MTX on parSlo + LRRC26 channels; the results are illustrated in Fig. 4.

Figure 4A shows an example of the voltage dependence of steady-state activation of parSlo + LRRC26 BK channels from the same cell before (○) and during treatment with 5 μM MTX (■). Unlike the very large 70-mV hyperpolarizing shift that MTX produced in cells without the LRRC26 protein (e.g., Fig. 2A), its presence was limited; in this case, the shift was ~19 mV. The mean V_h value for all six similarly treated cells was 35 ± 3.6 mV, and the mean shift produced by MTX was 17 mV. Figure 4B illustrates activation time constants obtained in the absence (○) and presence (■) of 5 μM MTX. A comparison of these data with those in Fig. 2B reveals that MTX had rather different effects on the activation kinetics of

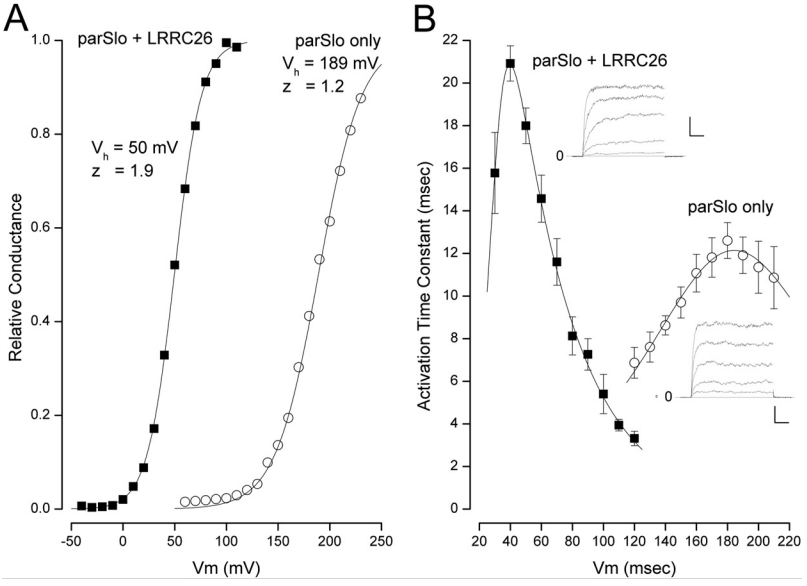

Fig. 3. Actions of LRRC26 on BK channel gating. A, voltage dependence of expressed parSlo channel conductance without (○, from Fig. 2A) and with (■) association with the LRRC26 protein. Solid lines, fits of the Boltzmann equation with the indicated parameters. B, voltage dependence of the channel activation time constant without (○, N = 5–19, from Fig. 2B) and with (■) the associated LRRC26 protein (N = 5). Solid lines are fits of eq. 1 to the data. Insets, raw currents from parSlo only and parSlo + LRRC26 channels as indicated. Currents from parSlo channels elicited by depolarizations from 140 to 220 mV in 20-mV increments; calibration, 1 nA/25 ms. Currents from parSlo + LRRC26 channels elicited by depolarizations from 20 to 100 mV in 20-mV increments; calibration, 2 nA/25 ms.

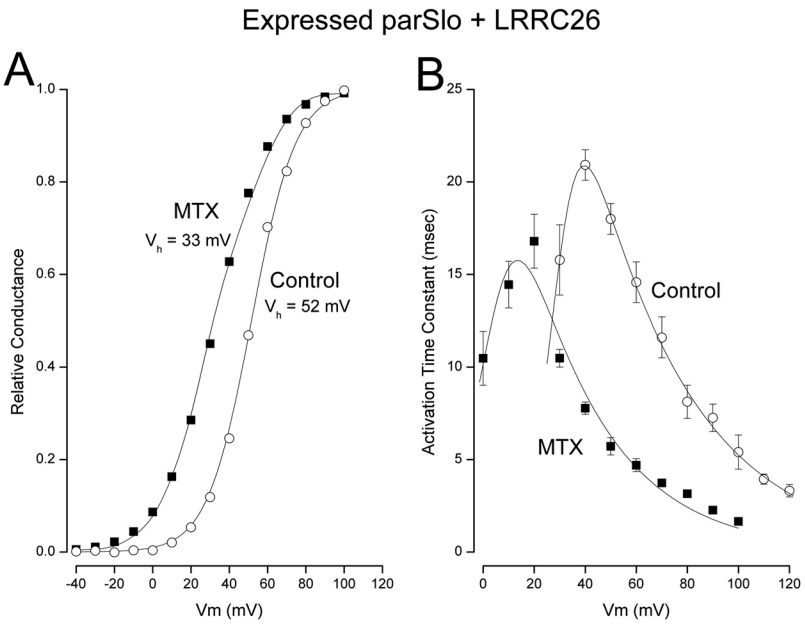

Fig. 4. MTX action on ParSlo + LRRC26 BK channels. A, voltage dependence of relative BK conductance in the absence (○) and presence (■) of 5 μM MTX. Solid lines, fits of the Boltzmann equation (see *Materials and Methods*) with the indicated parameters. B, voltage dependence of activation time constant in the absence (○, $N = 5$) and presence (■) of 5 μM MTX ($N = 4$ except $N = 3$ at 0 mV). Solid lines are fits of eq. 1 (see *Materials and Methods*) to the data.

BK channels with the LRRC26 protein than those without this accessory protein. Instead of a large, parallel shift of the voltage dependence of the time constants of parSlo-only channels (Fig. 2B), MTX produced a much smaller shift along with a decrease in the peak time constant of parSlo + LRRC26 BK channels. In summary, coexpression of LRRC26 with parSlo produced BK channels with intrinsic gating properties and sensitivity to MTX that reflected the properties of the channels in native parotid cells.

MTX Action on Heterologously Expressed parSlo BK Channels with High Internal Ca^{2+}. As shown in Figs. 1 and 4, MTX had a much smaller effect on steady-state activation of native and expressed parSlo + LRRC26 BK channels than on channels formed only of parSlo subunits (Fig. 2). The native and parSlo + LRRC26 channels have a much more hyperpolarized activation range than the parSlo-only channels. Thus, it is possible that the inability of MTX to produce a hyperpolarizing shift of the activation of these channels was due to their already negative activation range. We tested this idea by examining MTX action on expressed parSlo BK channels whose activation was shifted to more hyperpolarized potentials by inclusion of Ca^{2+} in the intracellular solution (Fig. 5).

Figure 5A shows that 10 μM internal Ca^{2+} caused expressed parSlo BK channels to activate at potentials even more negative than native BK channels or channels coexpressed with LRRC26. Nevertheless, MTX still produced a strong shift of channel activation to even more negative potentials. We found a mean V_h value of 35 ± 2 mV ($N = 10$) in the absence of MTX and a mean value of −3 ± 3 mV in the presence of 5 μM MTX. Thus, MTX was able to produce a 38-mV hyperpolarizing shift even of BK channels with an already hyperpolarized activation range—not as large as the 70-mV shift observed in zero Ca^{2+} but considerably larger

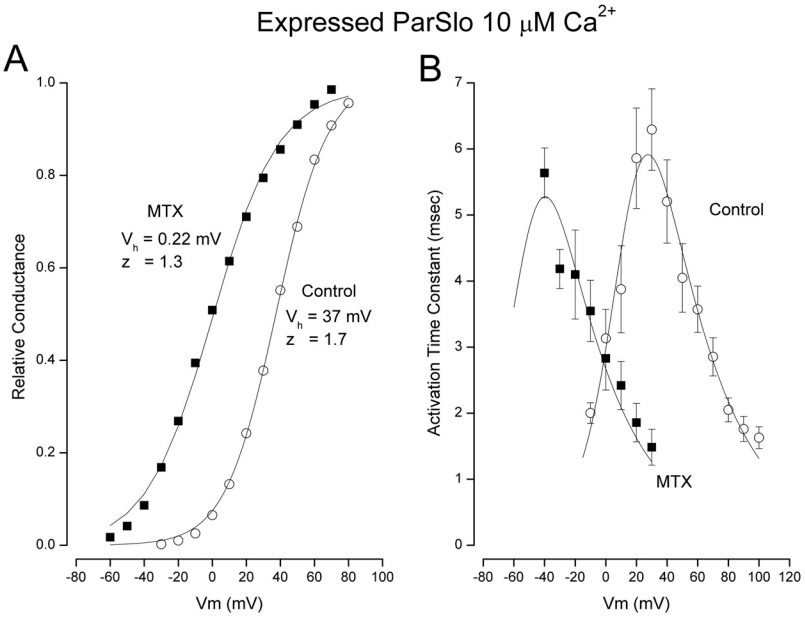

Fig. 5. MTX shifts expressed parSlo activation in high Ca^{2+}. A, voltage dependence of relative BK channel conductance from a cell in the absence (○) and presence (■) of 5 μM MTX. Solid lines, fits of the Boltzmann equation (see *Materials and Methods*) with the indicated parameters. B, voltage dependence of activation time constant in the absence (○, $N = 5$–7) and presence (■) of 5 μM MTX ($N = 4$–5). Solid lines are fits of eq. 1 (see *Materials and Methods*) to the data. All measurements were made with 10 μM intracellular Ca^{2+}.

than the shift of native BK channels or expressed parSlo + LRRC26 channels.

It should be noted that this finding complements the results from an analogous set of experiments by Zakharov et al. (2005). Those authors measured the ability of intracellular Ca^{2+} to shift BK channel activation in the presence of MTX, whereas we tested the efficacy of MTX in the presence of elevated Ca^{2+}. Their study was with cell-free, inside-out patches, whereas our results were obtained from intact cells. Nevertheless, we came to the same conclusion that the shifts produced by intracellular Ca^{2+} and MTX were independent of one another.

Figure 5B illustrates the voltage dependence of activation time constants in the absence (○) and presence (■) of 5 μM MTX in the presence of 10 μM Ca^{2+}. MTX seems to have produced mostly a simple, parallel hyperpolarizing shift of the voltage dependence of the activation time constant, reminiscent of its action on channels consisting of only the parSlo α-subunit. This conclusion is somewhat weakened by our lack of activation time constants in the presence of MTX at sufficiently negative potentials to visualize the maximal time constant value. However, the solid line, which provides a reasonable description of the MTX data, is the result of fitting eq. 1 to the data but with the constraints that the effective valance values (z_a and z_b) maintain their control values; in other words, a good fit was obtained by allowing only a simple shift of the voltage dependence.

The LRRC26 Accessory Protein and Other BK Channel Activators. As noted in the Introduction, there are several classes of BK channel activator compounds; a relevant question for this study was whether the LRRC26 interfered with BK activators other than MTX. Benzimidazalones such as NS-1619 are structurally very different from MTX, but both produce large hyperpolarizing shifts in BK channel activation. Gessner et al. (2005) found that NS-1619 caused a substantial shift of activation of BK channels in the LNCap prostate cell line. These channels contain the LRRC26 protein, suggesting that its ability to interfere with BK activators may not be universal. To specifically examine the role of LRRC26 on BK channel activation by NS-1619, we tested the effectiveness of NS-1619 on heterologously expressed parSlo channels and on parSlo channels expressed with the LRRC26 accessory protein; examples of the results are illustrated in Fig. 6.

Figure 6A contains voltage activation data measured in the nominal absence of Ca^{2+} from a cell expressing BK channels composed of only parSlo subunits in the absence (○) and presence (■) of 50 μM NS-1619. The V_h value for the activation in the absence of NS-1619 was 170 and 108 mV in its presence: a 62-mV hyperpolarizing shift. In a total of six similar experiments, the mean V_h value without NS-1619 was 181 ± 4.5 mV, similar to the values described above, and the mean hyperpolarizing shift produced by 50 μM NS-1619 was 61 ± 4.8 mV. Figure 6B shows that a somewhat smaller but still large shift is produced in channels with the LRRC26 protein. In the example shown, the V_h value for activation was 54 and 4 mV in the absence and presence of NS-1619, respectively. In a total of six similar experiments, the mean V_h value without NS-1619 was 51 ± 2.9 mV, similar to values described above, and the mean hyperpolarizing shift produced by 50 μM NS-1619 was 47 ± 3.2 mV. That is, the NS-1619-induced shift of BK channel activation was reduced by only 23% in the presence of the LRRC26 channel. In contrast, under similar conditions, the LRRC26 protein inhibited the MTX-induced gating shift by 76%.

Discussion

Several new findings have resulted from this study. In contrast to previous findings on smooth muscle BK channels, mallotoxin had very little effect on the voltage dependence of activation of BK channels in native parotid acinar cells. However, MTX was not entirely without effect as it produced a 2-fold increase in the speed of parotid BK channel activation. We showed that the limited action of MTX on the voltage dependence of BK channel activation in parotid cells was probably attributed to the existence of a BK channel accessory protein, LRRC26, which is expressed in salivary glands, including parotid (Egland et al., 2006; Gonzalez-Begne et al., 2009). Coexpression of parSlo with LRRC26 produced chan-

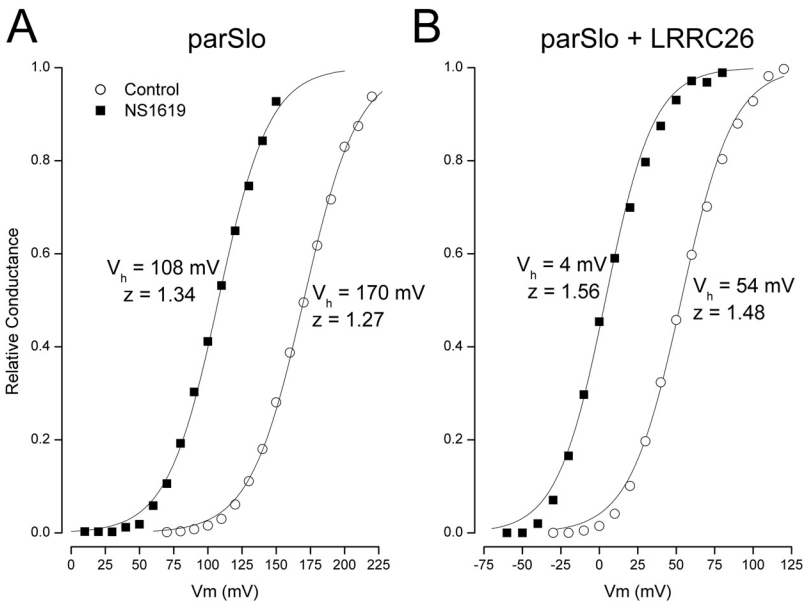

Fig. 6. NS-1619 on parSlo and parSlo + LRRC26 BK channels. A, voltage dependence of heterologously expressed parSlo BK channel conductance in the absence (○) and presence (■) of 50 μM NS-1619. B, voltage dependence of parSlo + LRRC26 BK channel conductance in the absence (○) and presence (■) of 50 μM NS-1619. Solid lines, fits of the Boltzmann equation (see *Materials and Methods*) with the indicated parameters.

nels that mimicked many of the properties of those in the native cells, including 1) a hyperpolarized activation range, 2) resistance to MTX modification of steady-state activation, and 3) a speeding of gating kinetics by MTX. We suggest that the relatively small differences between native parotid and parSlo + LRRC26 BK channels may be the result of an incomplete stoichiometry in the heterologous expression system. Finally, we showed that, although the LRRC26 protein inhibited the gating shift produced by MTX, it had a minimal effect on the gating shift produced by NS-1619. This result shows that the LRRC26 protein has a selective effect on BK channel pharmacology.

One possible mechanism for the inability of MTX to shift the voltage dependence of BK channels formed with the LRRC26 protein is that the accessory protein prevents binding of MTX to the channel complex. This does not seem to be the case because, even though MTX did not produce a significant activation shift of BK + LRRC26 channels, it did produce a substantial increase in the speed of activation of this BK channel complex (Figs. 1 and 4). The fact that MTX increased the kinetics of BK + LRRC26 channels but had no effect on the kinetics of BK channels without LRRC26 (Fig. 2) suggests another mechanism in which MTX displaces the LRRC26 protein reversing the slowing effect by the accessory protein and replacing the shift produced by LRRC26 by its own gating shift. The data in Figs. 1 and 3 show that this idea is quantitatively reasonable. The peak time constants of parotid and parSlo + LRRC26 channels were quite similar, and MTX caused the time constant of parSlo + LRRC26 channels to approach that of parSlo-only channels. Thus, the simple idea that MTX displaces the LRRC26 protein is quantitatively consistent with both the increase in activation kinetics and the minimal effect on the voltage dependence of activation of BK channels with the LRRC26 protein.

The Functional Basis for MTX and LRRC26 Action. More insight into the mechanism by which MTX and the LRRC26 protein compete could come from an understanding of the mechanisms by which they produce their large hyperpolarizing shifts of the BK activation process. The Horrigan-Aldrich allosteric model for BK channel activation provides a framework for analyzing the functional basis for the actions of LRRC26 and MTX. The full H-A model describes how voltage and Ca^{2+} act synergistically to control BK channel activation, but the actions of MTX and the LRRC26 protein were investigated in the nominal absence of Ca^{2+}. Under these conditions, the H-A model can be schematically represented as shown in Scheme 1. The overall channel open probability for Scheme 1 is given by eq. 2:

$$P_o = \frac{L(1 + JD)^4}{L(1 + JD)^4 + (1 + J)^4} \quad (2)$$

where

$$L = L_0 \exp\left(\frac{z_L V_m F}{RT}\right)$$

and

$$J = \exp\left(\frac{z_J F(V_m - V_J)}{RT}\right)$$

Thus, the Ca^{2+}-free version of the H-A model has five independent parameters: L_0, z_L, z_J, V_J, and D and the goal

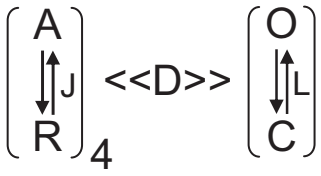

Scheme 1. The voltage sensors in each of the four BK channel subunits have a resting (R) and an activated (A) conformation controlled by a voltage-dependent equilibrium constant, J. The channel pore has a closed (C) and an open conducting (O) conformation governed by the voltage-dependent equilibrium constant L. There is a cooperative interaction between the voltage sensors and the pore represented by the D parameter.

then is to define the set of parameters that best describes measured activation data. At very negative potentials where the open probability is very small, P_o is simply equal to L, and so obtaining these data greatly improves the process of defining L_0 and z_L. These data can be obtained from measurements of single channel currents at negative potentials, which required the use of an external solution with an elevated level of K^+. Yan and Aldrich (2010) did this type of analysis on data from inside-out patches of cells expressing hSlo channels with and without the LRRC26 accessory protein. They found that their data from the BK-only channels could be well described by the H-A model with a set of parameters similar to those that have been reported previously. They went on to show that the data from channels with the LRRC26 protein could be accounted for if the allosteric coupling parameter D was greatly increased. We did a similar analysis of data from heterologously expressed parSlo channels in the absence and presence of MTX; the results are illustrated in Fig. 7.

Figure 7, ○, represents the voltage dependence of expressed parSlo channels, and the associated black lines are from our H-A model analysis with the indicated parameters (Basic Set). These values are within the range of those previously published for heterologously expressed mSlo, hSlo, and parSlo channels (Horrigan and Aldrich, 2002; Bao and Cox, 2005; Orio and Latorre, 2005; Wang et al., 2006; Romanenko et al., 2010; Yan and Aldrich, 2010).

Figure 7 also shows activation values for expressed parSlo channels treated with MTX (■), including values obtained from single channel measurements (see *Materials and Methods*) at very negative potentials. Although the data used for the analysis of the control data were pooled from many cells, the activation data in MTX at positive potentials are from a single representative cell (the data at negative potentials are from several cells). For reasons described under *Materials and Methods*, we believe that this approach allowed the most accurate estimation of the BK channel activation in the presence of MTX.

In the context of the H-A model, there are three general ways to produce a hyperpolarizing shift of activation: 1) a hyperpolarizing shift in the voltage sensor equilibrium (i.e., a more negative V_J value), 2) a hyperpolarizing shift in the open-closed equilibrium (i.e., a larger L_0 value), or 3) an increase in the coupling between voltage sensor activation and channel opening (i.e., an increase in D). The simulations illustrated in Fig. 7A demonstrate that no single one of these parameter changes could account for the action of MTX. A shift of V_J from 165 to 100 mV reproduced the data at positive potentials but was not with in an order of magnitude value of

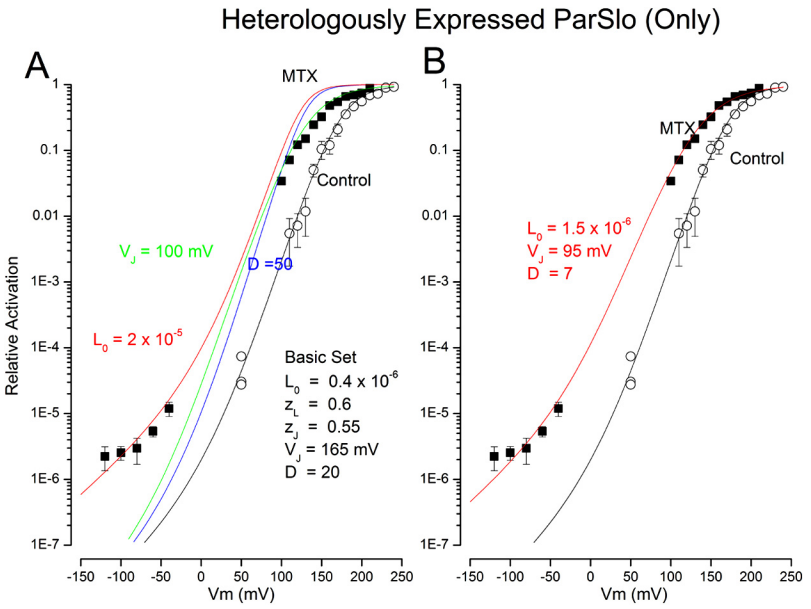

Fig. 7. H-A model simulations of the activation of expressed parSlo channels in the absence and presence of MTX. Voltage dependence of relative activation of heterologously expressed parSlo BK channels in the absence (○) and presence (■) of 5 μM MTX. Solid lines, simulation of the H-A model with the indicated parameters. Control data are pooled from several cells, $N = 4$ for $V_m \geq 140$ mV, $N = 3$ for V_m from 100 to 140 mV; data at +50 mV are single channel measurements from three individual cells. MTX data at large depolarizations are from a single cell with activation properties representative of the mean values of five cells. MTX data at negative voltages are mean values from six cells, with the exception of the value at −120 mV, which is the mean from three cells.

the data at the most negative voltages. A larger V_J shift would produce a better match to the data at negative potentials but would then not match the rest of the data. The increase in L_0 shown provides a good description of the negative voltage data but not of the data at depolarized potentials. As can be seen in the figure, no value of D was able to describe any part of the MTX data.

Thus, the MTX data could not be described by a change in any single aspect of BK channel gating. Indeed, we found that the only way to accurately describe the action of MTX was to allow all three parameters to change. Figure 7B shows that a modest increase in L_0 coupled with a 70-mV hyperpolarizing shift of V_J and a reduction in the coupling parameter D provided an accurate description of the MTX data. A reduction in D, on its own, would produce a depolarizing shift, so the changes in L_0 and especially V_J overcome this effect. Thus, it seems that MTX and the LRRC26 protein exert their actions on BK channel activation by quite different mechanisms. Our analysis indicates that MTX produces its shift primarily through a hyperpolarizing shift of the voltage sensor equilibrium voltage (V_J), whereas Yan and Aldrich (2010) concluded that LRRC26 produces its hyperpolarizing activation shift by increasing the allosteric coupling factor D.

Conclusion. BK channels are valuable targets for therapeutic interventions, and many compounds have been identified that modify BK channel gating. One such compound is MTX, which produces a large increase in the activation of smooth muscle BK channels. In contrast, we showed that MTX had only a minor effect on steady-state activation of BK channels in parotid acinar cells. We hypothesized that this was due to the presence in parotid cells of LRRC26, a protein known to produce a hyperpolarizing shift of BK channel activation and one that is expressed in these cells. We confirmed this hypothesis by showing that MTX was only weakly effective on steady-state activation of parotid BK channel isoform coexpressed with the LRRC26. We showed that the action of the LRRC26 protein was selective: it strongly interfered with the hyperpolarizing shift produced by MTX but had a minimal effect on the hyperpolarizing activation shift produced by the benzimidazalone BK activator NS-1619. We suggest that the ineffectiveness of the MTX on BK channels with the LRRC26 protein was the result of a competition between MTX and the LRRC26 protein for their action on the BK channel-gating machinery. It is presumed that the physical chemical properties of NS-1619 allow it to act independently of the LRRC26 protein. Indeed, Zakharov et al. (2005) showed that MTX shifts BK channel activation, even in the presence of NS-1619. Our results highlight the fact that the screening of BK channel drugs needs to include consideration for BK accessory proteins such as LRRC26 and that it may be possible to take advantage of this behavior to design tissue-specific BK channel-modifying drugs.

Acknowledgments

We are grateful for several discussions with Dr. Frank Horrigan on the details of the Horrigan-Aldrich model. We thank Jill Thompson for discussions on all aspects of this work and for critically reading the article. We thank James E. Melvin for discussions about the clinical relevance of BK channel activators for salivary gland fluid and electrolyte secretion. We also thank Dr. Robert Dirksen for critical comments on the article.

Authorship Contributions

Participated in research design: Begenisich and Almassy.
Conducted experiments: Almassy.
Performed data analysis: Begenisich and Almassy.
Wrote or contributed to the writing of the manuscript: Begenisich and Almassy.

References

Bao L and Cox DH (2005) Gating and ionic currents reveal how the BK_{Ca} channel's Ca^{2+} sensitivity is enhanced by its beta1 subunit. *J Gen Physiol* **126:**393–412.
Brayden JE and Nelson MT (1992) Regulation of arterial tone by activation of calcium-dependent potassium channels. *Science* **256:**532–535.
Butler A, Tsunoda S, McCobb DP, Wei A, and Salkoff L (1993) mSlo, a complex mouse gene encoding "maxi" calcium-activated potassium channels. *Science* **261:** 221–224.
Diaz L, Meera P, Amigo J, Stefani E, Alvarez O, Toro L, and Latorre R (1998) Role of the S4 segment in a voltage-dependent calcium-sensitive potassium (h*Slo*) channel. *J Biol Chem* **273:**32430–32436.
DiChiara TJ and Reinhart PH (1997) Redox modulation of h*slo* Ca^{2+}-activated K^+ channels. *J Neurosci* **17:**4942–4955.
Doyle DA, Morais Cabral J, Pfuetzner RA, Kuo A, Gulbis JM, Cohen SL, Chait BT, and MacKinnon R (1998) The structure of the potassium channel: molecular basis of K^+ conduction and selectivity. *Science* **280:**69–77.

Egland KA, Liu XF, Squires S, Nagata S, Man YG, Bera TK, Onda M, Vincent JJ, Strausberg RL, Lee B, et al. (2006) High expression of a cytokeratin-associated protein in many cancers. *Proc Natl Acad Sci USA* **103:**5929–5934.
Garcia ML, Giacobbe RA, Hensens OD, Kaczorowski GJ, Lee SH, McManus OB, and Zink DL (1995), inventors; Merck & Co., assignee. Biologically active compounds. U.S. patent 5,399,587. 1995 Mar 21.
Garcia ML, Goetz MA, Kaczorowski GJ, McManus OB, Monaghan RL, Strohl WR, and Tkacz JS (2007), inventors; Merck & Co., assignee. Maxi-K channel blockers, methods of use and process for making the same. U.S. patent 7,294,646. 2007 Nov 13.
Gessner G, Schönherr K, Soom M, Hansel A, Asim M, Baniahmad A, Derst C, Hoshi T, and Heinemann SH (2005) BK_{Ca} channels activating at resting potential without calcium in LNCaP prostate cancer cells. *J Membr Biol* **208:**229–240.
Gonzalez-Begne M, Lu B, Han X, Hagen FK, Hand AR, Melvin JE, and Yates JR (2009) Proteomic analysis of human parotid gland exosomes by multidimensional protein identification technology (MudPIT). *J Proteome Res* **8:**1304–1314.
Gribkoff VK, Starrett JE Jr, and Dworetzky SI (1997) The pharmacology and molecular biology of large-conductance calcium-activated (BK) potassium channels. *Adv Pharmacol* **37:**319–348.
Gribkoff VK, Starrett JE Jr, Dworetzky SI, Hewawasam P, Boissard CG, Cook DA, Frantz SW, Heman K, Hibbard JR, Huston K, et al. (2001) Targeting acute ischemic stroke with a calcium-sensitive opener of maxi-K potassium channels. *Nat Med* **7:**471–477.
Horrigan FT and Aldrich RW (1999) Allosteric voltage gating of potassium channels II. Mslo channel gating charge movement in the absence of Ca^{2+}. *J Gen Physiol* **114:**305–336.
Horrigan FT and Aldrich RW (2002) Coupling between voltage sensor activation, Ca^{2+} binding and channel opening in large conductance (BK) potassium channels. *J Gen Physiol* **120:**267–305.
Horrigan FT, Cui J, and Aldrich RW (1999) Allosteric voltage gating of potassium channels I. Mslo ionic currents in the absence of Ca^{2+}. *J Gen Physiol* **114:**277–304.
Ishii TM, Silvia C, Hirschberg B, Bond CT, Adelman JP, and Maylie J (1997) A human intermediate conductance calcium-activated potassium channel. *Proc Natl Acad Sci USA* **94:**11651–11656.
Jensen BS, Teuber L, Strobaek D, Christophersen P, and Olesen SP (2003), inventors; NeuroSearch A/S, assignee. Use of ion channel modulation agents. U.S. patent 6,525,043. 2003 Feb 25.
Jiang Y, Lee A, Chen J, Cadene M, Chait BT, and MacKinnon R (2002) Crystal structure and mechanism of a calcium-gated potassium channel. *Nature* **417:**515–522.
Latorre R, Oberhauser A, Labarca P, and Alvarez O (1989) Varieties of calcium-activated potassium channels. *Annu Rev Physiol* **51:**385–399.
Long SB, Campbell EB, and Mackinnon R (2005) Crystal structure of a mammalian voltage-dependent *Shaker* family K^+ channel. *Science* **309:**897–903.
Magleby KL (2003) Gating mechanism of BK (Slo1) channels: so near, yet so far. *J Gen Physiol* **121:**81–96.
Marx SO and Zakharov SI (2006), inventors; Trustees of Columbia University in the City of New York, Marx SO, and Zakharov SI, assignees. Use of rottlerin and its derivatives as activators of BK channel for therapy of hypertension and related disorders. World patent WO2006060196. 2006 Jun 8.
Nardi A and Olesen SP (2008) BK channel modulators: a comprehensive overview. *Curr Med Chem* **15:**1126–1146.
Nehrke K, Quinn CC, and Begenisich T (2003) Molecular identification of Ca^{2+}-activated K^+ channels in parotid acinar cells. *Am J Physiol Cell Physiol* **284:**C535–C546.
Orio P and Latorre R (2005) Differential effects of beta 1 and beta 2 subunits on BK channel activity. *J Gen Physiol* **125:**395–411.
Romanenko V, Nakamoto T, Srivastava A, Melvin JE, and Begenisich T (2006) Molecular identification and physiological roles of parotid acinar cell maxi-K channels. *J Biol Chem* **281:**27964–27972.
Romanenko VG, Nakamoto T, Srivastava A, Begenisich T, and Melvin JE (2007) Regulation of membrane potential and fluid secretion by Ca^{2+}-activated K^+ channels in mouse submandibular glands. *J Physiol* **581:**801–817.
Romanenko VG, Thompson J, and Begenisich T (2010) Ca^{2+}-activated K channels in parotid acinar cells: The functional basis for the hyperpolarized activation of BK channels. *Channels (Austin)* **4:**278–288.
Rothberg BS and Magleby KL (1999) Gating kinetics of single large-conductance Ca^{2+}-activated K^+ channels in high Ca^{2+} suggest a two-tiered allosteric gating mechanism. *J Gen Physiol* **114:**93–124.
Rothberg BS and Magleby KL (2000) Voltage and Ca^{2+} activation of single large-conductance Ca^{2+}-activated K^+ channels described by a two-tiered allosteric gating mechanism. *J Gen Physiol* **116:**75–99.
Salkoff L, Butler A, Ferreira G, Santi C, and Wei A (2006) High-conductance potassium channels of the SLO family. *Nat Rev Neurosci* **7:**921–931.
Stefani E, Ottolia M, Noceti F, Olcese R, Wallner M, Latorre R, and Toro L (1997) Voltage-controlled gating in a large conductance Ca^{2+}-sensitive K^+ channel (hslo). *Proc Natl Acad Sci USA* **94:**5427–5431.
Strøbaek D, Christophersen P, Holm NR, Moldt P, Ahring PK, Johansen TE, and Olesen SP (1996) Modulation of the Ca^{2+}-dependent K^+ channel, hslo, by the substituted diphenylurea NS 1608, paxilline and internal Ca^{2+}. *Neuropharmacology* **35:**903–914.
Teuber L, Christophersen P, Strobaek D, and Jensen BS (2003) inventors; Neurosearch A/S, assignee. Ion channel modulating agents comprising novel benzimidazolone derivatives. U.S. Patent 6,624,186. 23 Sep 2003.
Thompson J and Begenisich T (2006) Membrane-delimited inhibition of maxi-K channel activity by the intermediate conductance Ca^{2+}-activated K channel. *J Gen Physiol* **127:**159–169.
Thurm H, Fakler B, and Oliver D (2005) Ca^{2+}-independent activation of BK_{Ca} channels at negative potentials in mammalian inner hair cells. *J Physiol* **569:**137–151.
Wang B, Rothberg BS, and Brenner R (2006) Mechanism of beta4 subunit modulation of BK channels. *J Gen Physiol* **127:**449–465.
Yan J and Aldrich RW (2010) LRRC26 auxiliary protein allows BK channel activation at resting voltage without calcium. *Nature* **466:**513–516.
Zakharov SI, Morrow JP, Liu G, Yang L, and Marx SO (2005) Activation of the BK (SLO1) potassium channel by mallotoxin. *J Biol Chem* **280:**30882–30887.

Address correspondence to: Dr. Ted Begenisich, Department of Pharmacology and Physiology Box 711, University of Rochester Medical Center, Rochester, NY 14642. E-mail: ted_begenisich@URMC.rochester.edu